

Sol-gel transition of reversible cluster-cluster aggregations

Takamichi Terao and Tsuneyoshi Nakayama

Department of Applied Physics, Hokkaido University, Sapporo 060-8628, Japan

(Received 30 April 1998)

This paper investigates the sol-gel transition of reversible cluster-cluster aggregations in terms of numerical simulations. The temperature dependence of the sol-gel transition point c_g is calculated by forming clusters with different particle concentrations for two-dimensional ($d=2$) and three-dimensional ($d=3$) systems. We present phase diagrams on sol-gel transitions from these calculations. The fractal dimension D_f for $d=3$ reversible cluster-cluster aggregations is calculated at the sol-gel transition point, which gives $D_f=2.4\pm 0.1$, apparently larger than that of diffusion-limited cluster-cluster aggregations. These results show good agreement with those obtained by small-angle x-ray scattering experiments. [S1063-651X(98)15809-9]

PACS number(s): 61.43.Hv, 82.70.Gg, 82.20.Wt

I. INTRODUCTION

The aggregation processes of fine particles have attracted a great deal of interest in the past decade, due to their wide range of practical applications or their own scientific importances [1,2]. There are two types for aggregation processes. One is the particle-cluster aggregation [diffusion-limited aggregation (DLA)] proposed by Witten and Sander [3], for which the fractal dimension D_f becomes distinctly smaller than the Euclidean dimension d . This is a basic model for a variety of aggregations and other growth processes, in which only one particle is allowed in the vicinity of a growing cluster and all growth initiates from a collision between a single particle and a cluster. These features are, however, unrealistic for many actual colloidal systems. The other is the cluster-cluster aggregation model developed by Meakin [4] and Kolb, Botet, and Jullien [5], which describes the sol-gel transition due to a nonequilibrium process, whose underlying mechanism leading to the formation of gel networks has been far from complete. When the particle concentration c is larger than a characteristic gel concentration c_g , an aggregate spans a box from edge to edge in three directions and forms a gel network. Though several different models have been proposed to elucidate the formation of the gel network [6], the cluster-cluster aggregation model is the most successful one for understanding the gel formation.

The structural and kinetic characteristics of colloidal aggregations have been investigated by experiments and computer simulations [7,8], which have yielded a significant insight into the processes involved. It has been pointed out [9,10] that the interaction energy between particles plays an important role in the aggregation, namely, when the interaction energy is sufficiently strong, these aggregation processes become *irreversible*, and once particles (or clusters) are bonded together, they cannot break up. This aggregation process is called diffusion-limited cluster-cluster aggregation (DLCA), and it is known that this model describes well the structure of chemical gels such as silica aerogels [11,12]. Much research has been performed for the DLCA model, and various physical properties such as cluster-size distributions, kinetic gelations, and those vibrational dynamics have been investigated [4,5,11,13,14]. Numerical simulations indicate that the fractal dimensions of diffusion-limited cluster-

cluster aggregation take values of $D_f=1.44\pm 0.03$ for $d=2$ and $D_f=1.78\pm 0.06$ for $d=3$ [1].

There exist cases in which the effective attractive forces between particles (or clusters) are relatively weak or the temperature of the system is sufficiently high so that particles have high probability to escape from the cluster and break up. This aggregation process is *reversible*, i.e., particles are allowed to restructure within clusters or even break up from it. This model corresponds to physical gels, which have different properties from chemical gels described by the ordinary DLCA model. In the following, we refer to this aggregation as reversible cluster-cluster aggregation. Compared to the ordinary DLCA model, the physical properties of the reversible cluster-cluster aggregation model have not been clarified.

Reversible aggregations have been theoretically investigated by several authors [15–21]. Shih, Aksay, and Kikuchi [20] have performed computer simulations for the reversible cluster-cluster aggregation model on $d=2$, taking into account a finite attraction energy between particles. They have numerically studied the temporal evolution of clusters and the structure of aggregates, and demonstrated that the finite binding energy between particles changes the structure of aggregates. Jin *et al.* [21] have studied the gel formation on the model proposed by Shih, Aksay, and Kikuchi [20] on $d=2$, and found that the sol-gel transition point $c=c_g$ is non-zero and independent of the system size L when the interaction energy between particles is not very strong. However, there are few works on thermodynamic properties of reversible aggregations, and the understanding on these systems is far from complete. Especially, direct numerical investigations on $d=3$ reversible cluster-cluster aggregations are lacking to clarify the gel formation processes in actual materials such as colloidal aggregations.

In this paper, the sol-gel transition of the reversible cluster-cluster aggregation model is numerically studied. The sol-gel transition point c_g and its temperature dependence are determined by forming clusters on a $d=2$ square lattice and a $d=3$ simple-cubic lattice, by changing particle concentrations. From these calculations, phase diagrams for sol-gel transitions are obtained for $d=2$ and $d=3$ systems. In addition, the fractal dimension D_f of aggregates on the sol-gel transition point is obtained as $D_f=2.4\pm 0.1$, which is appar-

ently larger than that of the $d=3$ DLCA model. This result agrees well with results by small-angle light and x-ray scattering experiments.

II. MODELS

We describe the formation rules of the reversible cluster-cluster aggregation, in the system of units $a=1$ for a lattice constant [4,5,20]. In this model, N particles are randomly disposed in a cubic box of the size L , where the particle concentration is $c \equiv N/L^3$. The i th particle (or cluster) is chosen at random according to the probability $P(n_i, \alpha)$ defined by

$$P(n_i, \alpha) \equiv \frac{n_i^\alpha}{\sum_i n_i^\alpha}, \quad (1)$$

where n_i is the number of particles in the i th cluster and α is a numerical parameter. The i th cluster is moved by one step along a randomly chosen direction among six directions $(\pm 1, 0, 0)$, $(0, \pm 1, 0)$, $(0, 0, \pm 1)$ in a cubic box. If the cluster does not collide with another one, the displacement is performed and the algorithm goes on by choosing again another cluster. When two clusters collide, they stick together forming a new large cluster, and another cluster is chosen again at random.

Here the total energy of the system E is defined as a summation of all binding energies between nearest-neighbor particles such as

$$E \equiv \sum_{\langle m, n \rangle} \epsilon_{mn}, \quad (2)$$

where ϵ_{mn} is the interaction energy between particles m and n , which is given by $\epsilon_{mn} = -\epsilon$ ($\epsilon > 0$) if particles m and n are nearest-neighbor, otherwise $\epsilon_{mn} = 0$. The particles are allowed to rearrange their positions within the same cluster or break apart from it, which is different from the ordinary DLCA model. The probability p_b of such moves depends on the difference of the total energy of the system ΔE due to this process, which is given by

$$p_b = \begin{cases} 1 & \text{for } \Delta E < 0, \\ \exp(-\Delta E/k_B T) & \text{for } \Delta E \geq 0, \end{cases} \quad (3)$$

where k_B and T are the Boltzmann constant and a temperature of the system, respectively. For detailed algorithm of this model, see Ref. [20]. This procedure is repeated until the total energy of the system E approaches a constant value. After sufficiently long time steps, the system reaches a thermal equilibrium state.

III. NUMERICAL RESULTS

At first, we construct reversible cluster-cluster aggregations by means of computer simulations, where the clusters are formed on a $d=2$ square lattice and a $d=3$ simple-cubic lattice, under periodic boundary condition in all spatial directions. The interaction energy ϵ between nearest-neighbor particles [see Eq. (2)] is taken as $\epsilon=1$. In the following, the parameter α in Eq. (1) is chosen as $\alpha=0$ for simplicity [14]. The calculations with the parameter $\alpha=-0.42$ are also per-

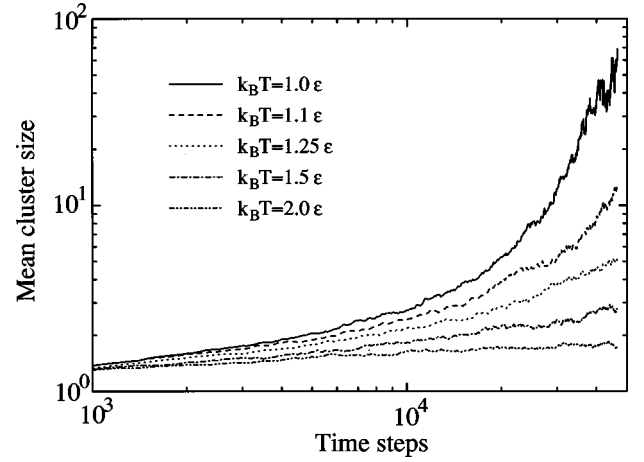


FIG. 1. The time development of the mean-cluster size for five different temperatures ($k_B T/\epsilon=1.0, 1.1, 1.25, 1.5$, and 2.0) for the $d=3$ system. The system size L and the particle concentration c are taken as $L=30$ and $c=0.04$, respectively.

formed to confirm our numerical results [22], which give the same conclusion as the case for $\alpha=0$.

Figure 1 shows the time development of the mean cluster size on the $d=3$ system for five different temperatures ($k_B T/\epsilon=1.0, 1.1, 1.25, 1.5$, and 2.0). The system size L and the particle concentration c are taken as $L=30$ and $c=0.04$, respectively. At smaller time steps ($\leq 5 \times 10^4$), the system does not approach an equilibrium state. Figure 1 shows such a tendency that the mean cluster size becomes larger as the temperature decreases. This result reflects the fact that the mean cluster size diverges at the sol-gel transition point.

Figure 2 shows the time dependence of the total energy E of $d=3$ reversible cluster-cluster aggregations for three different temperatures ($k_B T/\epsilon=1.0, 1.5$, and 2.0), where E is defined by Eq. (2). The system size L and the particle concentration c are taken as the same values as those in Fig. 1. After $\sim 10^5$ time steps, the total energy E becomes approximately constant at each temperature as seen from Fig. 2,

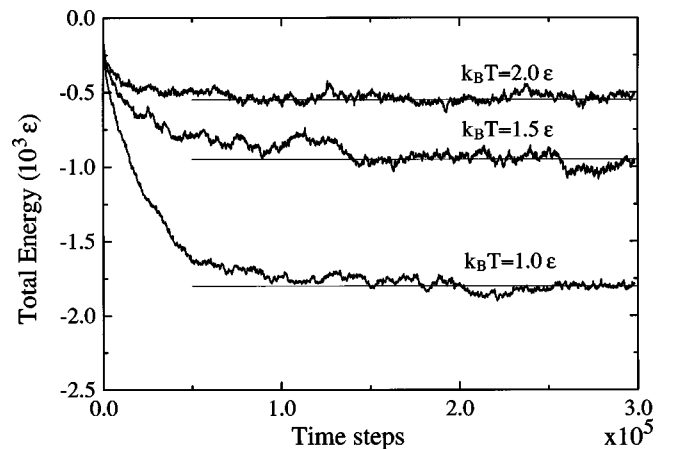


FIG. 2. The time dependence of the total energy E for three different temperatures ($k_B T/\epsilon=1.0, 1.5$, and 2.0) for the $d=3$ system, where E is defined by Eq. (2). The system size L and the particle concentration c are taken as $L=30$ and $c=0.04$, respectively. Horizontal lines are only guides for the eye.

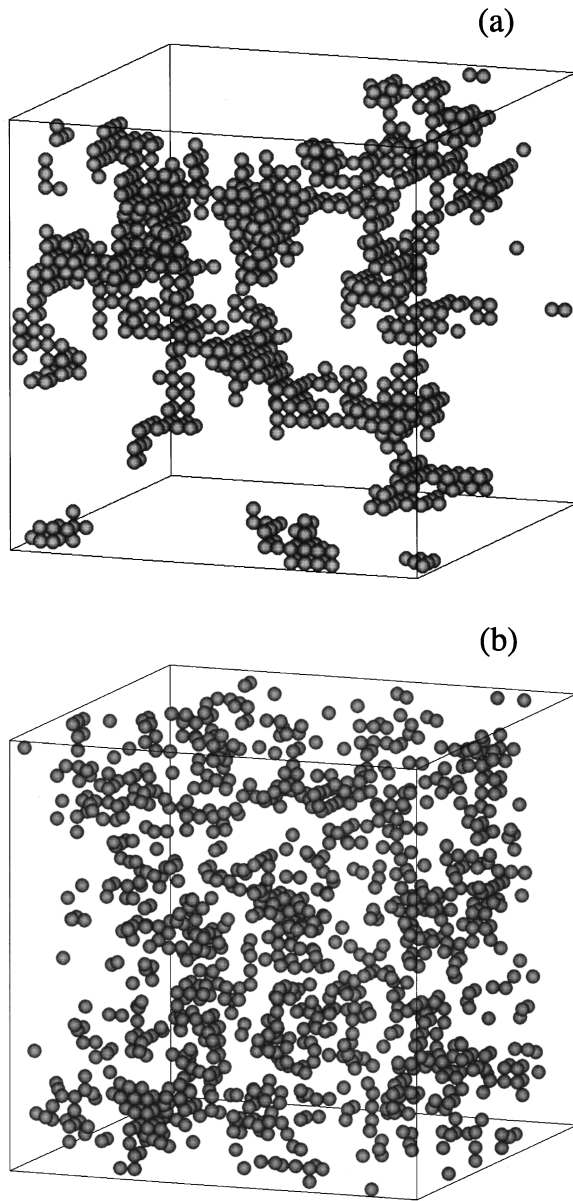


FIG. 3. (a) Three-dimensional reversible cluster-cluster aggregation formed on a simple-cubic lattice. The system size and the particle concentration are taken as $L=30$ and $c=0.04$, respectively. The temperature is taken to be $k_B T=0.1\epsilon$. (b) Three-dimensional reversible cluster-cluster aggregation formed on a simple-cubic lattice. The system size and the particle concentration are taken as $L=30$ and $c=0.04$, respectively. The temperature is taken to be $k_B T=2.0\epsilon$.

indicating that the system reaches an equilibrium state. Figure 2 confirms that sufficiently long time steps are taken to study behaviors of cluster-cluster aggregations at thermal equilibrium.

Figures 3(a) and 3(b) show snapshots of $d=3$ reversible cluster-cluster aggregations formed on a simple-cubic lattice, after sufficiently long time steps ($\geq 2 \times 10^5$). In Fig. 3(a), the system size and the particle concentration are taken as $L=30$ and $c=0.04$, respectively, and the temperature is chosen to be $k_B T=0.1\epsilon$. In Fig. 3(b), the system size and the particle concentration are the same as those in Fig. 3(a), and the temperature is chosen to be $k_B T=2.0\epsilon$. At lower tem-

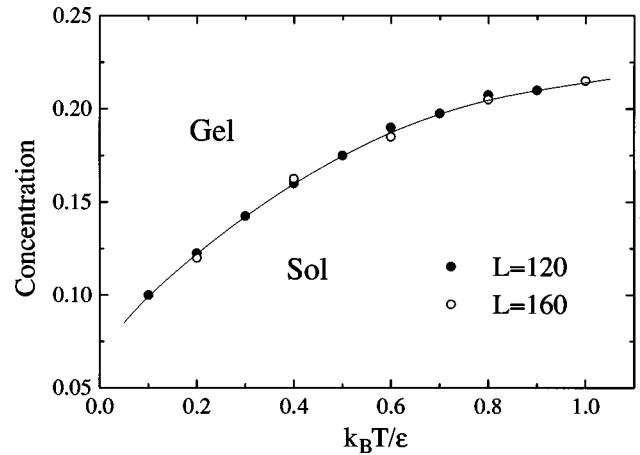


FIG. 4. Phase diagram of reversible cluster-cluster aggregation formed on a $d=2$ square lattice. Solid circles and open circles show the results for $L=120$ and 160 , respectively. The binding energy between particles ϵ is taken as $\epsilon=1$.

perature [Fig. 3(a)], the maximum cluster spans from end to end in a box and forms a gel network. On the contrary, we see that at higher temperature [Fig. 3(b)], a lot of small clusters exist in a box and do not form a gel network, though the concentration of the particles c is the same between these two different systems. These calculated results indicate that the sol-gel transition depends on temperature T .

Figure 4 shows the calculated results on the phase diagram of reversible cluster-cluster aggregations formed on a $d=2$ square lattice. We have computed 120 samples for each set of particle concentration and temperature, and the gelation point $c_g = c_g(T)$ is determined as the value c for which half of all the calculated samples form a gel network [21]. We have investigated the properties of aggregates with two different system sizes L . In Fig. 4, solid circles and open circles indicate the sol-gel phase boundaries with $L=120$ and 160 , respectively. Results with different system sizes show good agreement, indicating that the sol-gel transition point $c = c_g$ on reversible cluster-cluster aggregation does not depend on the system size at sufficiently high temperature, which has been pointed out for a $d=2$ system [21]. This result shows that the value of $c_g = c_g(T)$ becomes larger with increasing temperature of the system.

Figure 5 shows the phase diagram of reversible cluster-cluster aggregations formed on a $d=3$ cubic lattice. Solid and open circles show the numerical results on c_g for the system size $L=30$ and 36 , respectively. In these calculations, the number of time steps is taken to be over 2.4×10^5 for $L=30$ and 5×10^5 for $L=36$ to construct each aggregation, since much longer time steps are necessary to approach thermal equilibrium with increasing system sizes. This result is consistent with Figs. 3(a) and 3(b), implying that, at the particle concentration $c=0.04$, there is a sol-gel transition between temperatures $k_B T=0.1\epsilon$ and 2.0ϵ on three-dimensional system. To our knowledge, this is the first observation of the sol-gel transition and its phase-diagram for $d=3$ reversible cluster-cluster aggregations in terms of computer simulations.

In Fig. 6, the number of particles of the maximum cluster N_{\max} is plotted against R_g on a log-log scale, where R_g is the gyration radius of the cluster in units of a lattice constant.

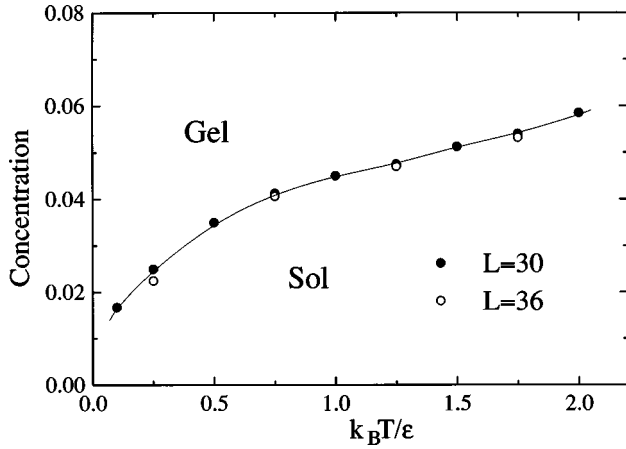


FIG. 5. Phase diagram of reversible cluster-cluster aggregation formed on a $d=3$ simple-cubic lattice. Solid circles and open circles show the results for $L=30$ and 36 , respectively. The binding energy between particles ϵ is taken as $\epsilon=1$.

The gyration radius R_g is defined as [23],

$$R_g \equiv \frac{1}{2N_{\max}^2} \sum_{i,j=1}^{N_{\max}} |\mathbf{r}_i - \mathbf{r}_j|, \quad (4)$$

where \mathbf{r}_i denotes the positional vector of the i th particle. The particle concentration and the temperature are chosen to be $c=0.058$ and $k_B T=2.0\epsilon$, respectively. These parameters correspond to the sol-gel transition point $c=c_g(T)$ on the $d=3$ system (see Fig. 5). The fractal dimension D_f of reversible cluster-cluster aggregations can be obtained from the relationship between the number of particle N_{\max} and the gyration radius R_g such as

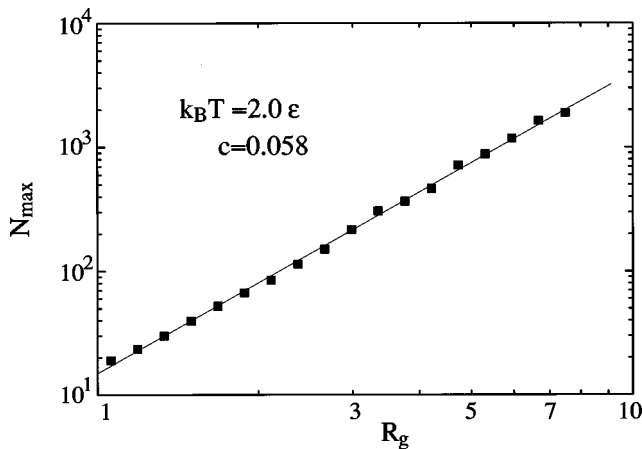


FIG. 6. The relationship between N_{\max} and R_g at the sol-gel transition point, where N_{\max} is the size of a maximum cluster and R_g is its gyration radius in units of a lattice constant $a=1$. The temperature and the particle concentration are taken as $k_B T=2.0\epsilon$ and $c_g=0.058$, respectively.

$$N_{\max} \propto R_g^{D_f}. \quad (5)$$

From Fig. 6, the value of D_f is found to be $D_f=2.4\pm 0.1$ by the least-squares fitting, which is apparently larger than that of the $d=3$ diffusion-limited cluster-cluster aggregation model ($D_f=1.78\pm 0.06$). This difference is due to the restructuring effect of aggregations [9,10,20]. By performing repeatedly in a temporal sequence small-angle-scattering measurements on colloidal aggregations, it has been found that colloidal aggregates with an initially lower fractal dimension ($D_f\approx 1.75$) restructure having a higher D_f (≈ 2.08 [9] and 2.4 [10]) at a later time. These experiments clearly indicate that a reversibility plays an important role in the growth process. Our results have demonstrated that the structure of the aggregates shows fractality during restructuring, and the fractal dimension D_f depends on the reversible nature of aggregation processes. Though these calculations are performed on lattice systems, it would not affect our conclusions because of universality. This feature is in good agreement with experimental results [9,10].

IV. CONCLUSIONS

To summarize, we have performed computer simulations on reversible cluster-cluster aggregations, which is known to be a successful model for the gel formation. Especially, we have concentrated on the sol-gel transition of reversible cluster-cluster aggregations, i.e., the model of physical gels in which the finite binding energy between particles plays an important role. With allowing particles to restructure within clusters or break up from them, the aggregates have been formed on a square lattice and a simple-cubic lattice by changing particle concentrations and temperatures. For forming aggregates, it has been experimentally observed that the size of the clusters increases at the first stage. After sufficiently long time steps, the total energy of the system becomes approximately constant, indicating that the system reaches thermal equilibrium. At higher temperatures, small clusters are distributed in a box and they do not form a gel network. With decreasing the temperature of the system, the size of the clusters increases rapidly, and at lower temperatures a cluster spans from end to end in a box and forms a gel network. This indicates that the sol-gel transition depends on the temperature T . We have obtained, from these calculations on the sol-gel transition point $c_g=c_g(T)$, phase diagrams for a $d=2$ square lattice and a $d=3$ simple-cubic lattice as a function of a particle concentration c and the temperature T .

We have found that there is a nonzero sol-gel transition point $c=c_g$ being independent of the system size L , which is consistent with the previous studies on $d=2$ systems [21]. It has been also observed that the value of c_g becomes larger as the temperature of the system increases. In addition, the relationship between the particle number in the maximum cluster N_{\max} and its gyration radius R_g has been investigated, and the fractal dimension D_f for $d=3$ reversible cluster-cluster aggregations is calculated at the sol-gel transition point. This takes $D_f=2.4\pm 0.1$, which is apparently larger than that of the $d=3$ DLCA model with $D_f\approx 1.78$. Our results indicate

that aggregates clearly take fractal structure during the restructuring process and the value of fractal dimension D_f changes due to the reversible nature of the aggregation process, which is in good agreement with the results of small-angle-scattering experiments on colloidal aggregations. Our work will shed light on the thermodynamic properties of cluster-cluster aggregations over a wide range of experimental conditions [7–10].

ACKNOWLEDGMENTS

This work was supported in part by a Grant-in-Aid from the Japan Ministry of Education, Science, and Culture for Scientific Research in Priority Areas, Cooperative Phenomena in Complex Liquid. The authors thank the Supercomputer Center, Institute of Solid State Physics, University of Tokyo, for the use of their facilities.

-
- [1] T. Vicsek, *Fractal Growth Phenomena* (World Scientific, Singapore, 1989).
 - [2] A. Erzan, L. Pietronero, and A. Vespignani, *Rev. Mod. Phys.* **67**, 545 (1995).
 - [3] T. A. Witten and L. M. Sander, *Phys. Rev. Lett.* **47**, 1400 (1981).
 - [4] P. Meakin, *Phys. Rev. Lett.* **51**, 1119 (1983).
 - [5] M. Kolb, R. Botet, and R. Jullien, *Phys. Rev. Lett.* **51**, 1123 (1983).
 - [6] F. Family and D. P. Landau, *Kinetics of Aggregation and Gelation* (North-Holland, Amsterdam, 1984).
 - [7] D. J. Robinson and J. C. Earnshaw, *Phys. Rev. A* **46**, 2045 (1992), and references therein.
 - [8] M. Carpineti and M. Giglio, *Phys. Rev. Lett.* **70**, 3828 (1993).
 - [9] C. Aubert and D. S. Cannel, *Phys. Rev. Lett.* **56**, 738 (1986).
 - [10] P. Dimon, S. K. Sinha, D. A. Weitz, C. R. Safinya, G. S. Smith, W. A. Varady, and H. M. Lindsay, *Phys. Rev. Lett.* **57**, 595 (1986).
 - [11] A. Hasmy, E. Anglaret, M. Foret, J. Pelous, and R. Jullien, *Phys. Rev. B* **50**, 6006 (1994).
 - [12] E. Anglaret, A. Hasmy, E. Courtens, J. Pelous, and R. Vacher, *Europhys. Lett.* **28**, 591 (1994).
 - [13] A. Rahmani, C. Benoit, R. Jullien, G. Poussigue, and A. Sakout, *J. Phys.: Condens. Matter* **8**, 5555 (1996).
 - [14] T. Terao, A. Yamaya, and T. Nakayama, *Phys. Rev. E* **57**, 4426 (1998).
 - [15] J. D. Barrow, *J. Phys. A* **14**, 729 (1981).
 - [16] R. M. Ziff and E. D. McGrady, *J. Phys. A* **18**, 3027 (1985).
 - [17] M. H. Ernst and P. G. J. van Dongen, *Phys. Rev. A* **36**, 435 (1987).
 - [18] F. Family, P. Meakin, and J. M. Deutch, *Phys. Rev. Lett.* **57**, 727 (1986).
 - [19] M. Kolb, R. Botet, R. Jullien, and H. J. Herrmann, in *On Growth and Form*, edited by H. E. Stanley and N. Ostrowsky (Nijhoff, Dordrecht, 1986), p. 222; M. Kolb, *J. Phys. A* **19**, L263 (1986).
 - [20] W. Y. Shih, I. A. Aksay, and R. Kikuchi, *Phys. Rev. A* **36**, 5015 (1987).
 - [21] J.-M. Jin, K. Parbhakar, L. H. Dao, and K. H. Lee, *Phys. Rev. E* **54**, 997 (1996).
 - [22] The value of α in Eq. (1) is taken to be $\alpha = -1/D_f$ in some previous studies, in order to insure that the diffusion coefficient of aggregates varies with the inverse of their radius.
 - [23] D. Stauffer and A. Aharony, *Introduction to Percolation Theory*, 2nd ed. (Taylor & Francis, London, 1992).